A Tricyclic Aromatic Isomer of Hexasilabenzene

Kai Abersfelder, *et al.*

Science **327**, 564 (2010);
DOI: 10.1126/science.1181771

A Tricyclic Aromatic Isomer of Hexasilabenzene

Kai Abersfelder, Andrew J. P. White, Henry S. Rzepa,* David Scheschkewitz*

Benzene represents the showcase of Hückel aromaticity. The silicon analog, hexasilabenzene, has consequently been targeted for decades. We now report an intensely green isomer of Si_6R_6 (R being 2,4,6-triisopropylphenyl) with a tricyclic structure in the solid state featuring silicon atoms with two, one, and no substituents outside the ring framework. The highly dispersed ^{29}Si nuclear magnetic resonance shifts in solution ranging from +125 to −90 parts per million indicate an inhomogeneous electron distribution due to the dismutation of formal oxidation numbers as compared with that of benzene. Theoretical analysis reveals nonetheless the cyclic delocalization of six mobile electrons of the π-, σ- and non-bonding type across the central four-membered ring. For this alternative form of aromaticity, in principle applicable to many Hückel aromatic species, we propose the term dismutational aromaticity.

Benzene has stimulated synthetic and theoretical chemists since its discovery by Faraday in 1825 (*1*). It provided the basis for the famous rule associated with Hückel that the presence of $4n + 2$ cyclically delocalized π-electrons implies aromaticity and related stabilization (*2*). Controversies regarding the concept continue to this day to provoke much productive research (*3*). Not surprisingly, the potential energy surface (PES) of C_6H_6 is one of the best studied. More than 200 isomers have been identified, all being at least 60 kcal mol^{-1} higher in energy than benzene (*4*).

The prospect of aromaticity in compounds involving silicon was ignored for a long time because silicon was generally considered unable to form stable π-bonds (*5*). However, in 1981 West *et al*. reported a stable disilene, a compound with a Si-Si double bond sterically protected by bulky mesityl (2,4,6-trimethylphenyl) groups (*6*). Since then, about 100 disilenes (*7*) and even a few compounds with Si-Si triple bonds (*8*, *9*) have been isolated, taking advantage of steric and/or electronic stabilization.

Cyclically delocalized π-systems involving silicon shifted into focus (*10*), and numerous breakthroughs have been achieved, such as the isolation of stable sila- and 1,2-disilabenzenes with planar, Hückel-aromatic structures (*11*, *12*). Potentially aromatic compounds based on silicon alone are so far limited to persila-analogs of cyclopropenium cation (*13*) and cyclobutadiene dianion (*14*).

Because of the special role of benzene, a particularly enticing sila-aromatic compound is the elusive hexasilabenzene. After early predictions of a sixfold symmetry analogous to that of benzene (*15*), a chair-like confirmation resembling that of cyclohexane was established through theoretical calculations (*16*, *17*). Experimentally, only an isomeric, nonaromatic hexasilaprismane has been prepared by the reduction of a 1,1,2,2-tetrahalodisilane (*18*), suggesting that the choice of precursor may be important in any synthetic approach.

A way to prearrange half of the Si_6-scaffold became apparent to us in light of our previous results concerning the reaction of disilenide **1** with an excess of dichlorosilanes affording cyclotrisilanes (*19*).

Extrapolating these results to silicon tetrachloride ($SiCl_4$), we anticipated that cyclotrisilane **2** may become accessible, although the reaction of **1** with a shortage of $SiCl_4$ yields a Si_5Tip_6-cluster (*20*). Conversely, rapid addition of an excess of $SiCl_4$ to disilenide **1** (*21*) afforded **2** in 59% isolated yield (Scheme 1) (*22*). Given the unsymmetric 1,1,2-substitution pattern of **2** (confirmed by means of x-ray diffraction) (figs. S2 to S4) (*22*), we expected it to provide an alternative entry to Si_6R_6 chemistry. Reduction of **2** with three equivalents of lithium/naphthalene in tetrahydrofuran/diethylether (3:5 ratio) led to the product **3a** (R being 2,4,6-triisopropylphenyl, or Tip), which was isolated as dark green crystals in 52% yield (Scheme 1) (*22*). The surprisingly stable **3a** can be exposed to air for hours as a solid or for minutes in solution without detectable changes. Melting-associated decomposition was observed at 216°C.

The highest mass in the mass spectrum of **3a** is observed at 1388 mass/charge ratio (*m*/*z*) with the correct isotopic distribution for $Si_6C_{90}H_{138}$ indicating the formation of a dimeric structure. On the basis of a two-dimensional $^{29}Si/^{1}H$ nuclear magnetic resonance (NMR) correlation, the ^{29}Si NMR signals at 124.6, −84.8, and −89.3 parts per million (ppm) were assigned to two silicon atoms each with one, two, and no directly attached Tip

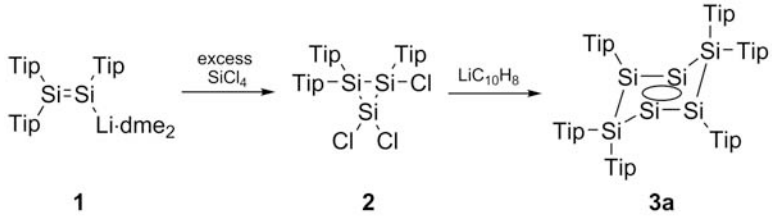

Scheme 1. Synthesis of the dismutational hexasilabenzene isomer **3a** (Tip, 2,4,6-triisopropylphenyl).

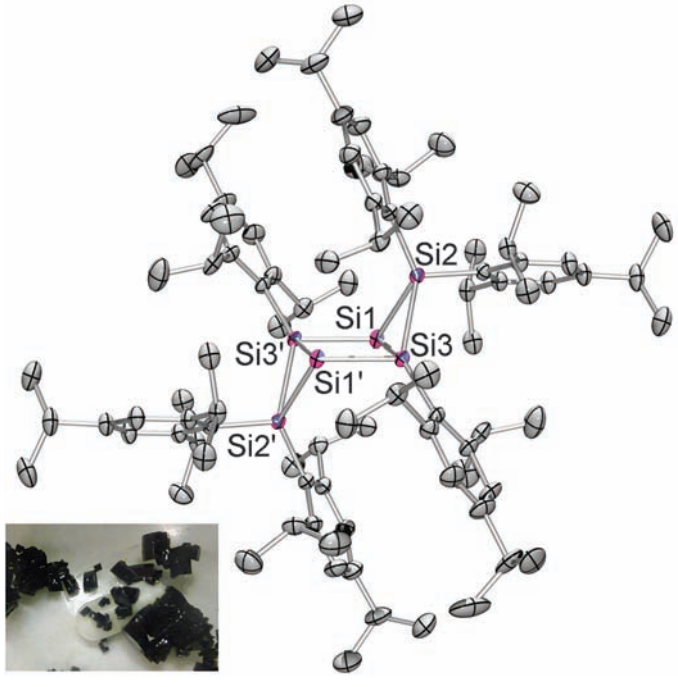

Fig. 1. Structure of **3a**·$2C_{10}H_8$ (thermal ellipsoids at 50%). Hydrogen atoms and naphthalene molecules are omitted for clarity. (Insert) Photographic image of dark-green crystals of **3a**·C_6H_6. Selected bond lengths in angstroms (estimated SD) are Si1-Si2 = 2.3581 (5), Si1-Si3 = 2.3275(5), Si1-Si3′ = 2.3034(5), Si1-Si1′ = 2.7287(7), and Si2-Si3 = 2.3375(5).

Imperial College London, Department of Chemistry, London SW7 2AZ, UK.

*To whom correspondence should be addressed. E-mail: d.scheschkewitz@imperial.ac.uk (D.S.); rzepa@imperial.ac.uk (H.S.R.)

substituent, respectively. The most positive ^{29}Si NMR chemical shift is observed in the region typical for tetrasilyl-substituted Si=Si bonds (*7*) and far from the negative region where signals of tetracoordinate silicon atoms within small rings are found (*18*–*20*). This observation excluded any saturated structure as a possible product. The green color of **3a**, due to the longest wavelength absorption in the ultraviolet (UV)/vis spectrum at λ = 623 nm, would also be highly atypical of saturated silicon compounds.

An x-ray diffraction study on single crystals of **3a** confirmed the features deduced from the spectroscopic data (Fig. 1) (*22*). The hexasilabenzene isomer **3a** crystallizes as a naphthalene solvate (**3a**·2 $C_{10}H_8$). Despite its tricyclic connectivity, the chair-like conformation of **3a** resembles the predicted puckered structure of hexasilabenzene (*16*, *17*). **3a** exhibits a rhomboid Si_4-ring in the center (Si1, Si3 and symmetry equivalents Si1′, Si3′), with two opposing $SiTip_2$ bridges (Si2, Si2′) pointing up- and downwards with respect to the Si_4 plane [the angle to Si1-Si2-Si3 is 66.80(2)°, with estimated SD in parentheses]. Si1 and Si1′ show hemispherical coordination; all bonds point into one-half of an imaginary sphere, which is a common coordination in case of lead (*23*), tin, and germanium (*24*) but rare for neutral silicon compounds (*20*, *25*). Despite the $SiTip_2$ bridges, Si1-Si3 [2.3275(5) Å] is only slightly longer than Si1-Si3′ [2.3034(5) Å], both being at the shorter end of typical Si-Si single bonds. The rhomboidal distortion becomes apparent in one shorter diagonal distance [Si1-Si1′ 2.7287(7) Å], which nonetheless is almost 17% longer than typical Si-Si single bonds.

On the basis of the analytical data, a resonance hybrid between **A** and **B** seemed best suited to describe the electronic structure of **3a** (Scheme 2). Contrasting the usual six π-electrons of Hückel aromatic systems, the mobile electrons in **3a** would nominally be of three different types. Two π-, two σ-, and two nonbonding electrons could be cyclically delocalized over four silicon centers with formal interruption of the σ-framework by two saturated $SiTip_2$ homobridges (*26*). Because of the topological similarities to singlet diradicals of the Niecke type (*27*), however, we initially did not exclude a certain diradical character in **3a** (resonance form **C**).

Density functional theory (DFT) calculations (*22*) on the Dip-substituted model compound **3b** (R being 2,6-diisopropylphenyl, or Dip) at the B3LYP/6−31G(d)–level of theory clarified the bonding situation (interactive table). The experimental geometry of **3a** is reasonably well reproduced despite substitution of the *para*-isopropyl groups with hydrogen atoms [for example, diagonal distance **3b**: Si1-Si1′ 2.779Å (calculated), 2.7287(7) (observed) Å]. The experimental trends in the ^{29}Si NMR shifts of **3a** agree well with those calculated for the model compound **3b** [δ = 170, −46, and −83 ppm, B3LYP/6-311+G(2df) basis on Si; 6-31G(d) on C,H]. Additionally, the UV/vis spectrum of **3b** simulated with time-dependent DFT (TDDFT) calculations is very similar to the experimental spectrum of **3a**. The closed-shell model **3b** appeared justified by the conformity of experiment and theory, which we lent further support by optimization of the triplet ^3A_u state of **3b**, revealing a much longer diagonal distance (3.069 Å) between the substituent-free silicon atoms. The adiabatic singlet-triplet gap of $E_{S\text{-}T}$ = 24.1 kcal mol^{-1} and the dominant (>90%) contribution of a single closed-shell configuration to the complete active space self-consistent field (CASSCF) (8,8) computed multireference wave function for the parent model (**3c**, using the Si geometry computed for **3b**) supports a low diradical character for **3b** (*28*).

Inspection of the relevant molecular orbitals (MOs) of **3b** (Fig. 2 and interactive table) reveals that the highest occupied molecular orbital (HOMO) (orbital 309), HOMO−2, and HOMO−3 (the dismutative trio) are all cyclically delocalized around the central Si_4 ring. The HOMO−3 is also conjugated with the aryl rings of four of the Dip groups (which is characteristic of π-aromatic bonds). In contrast, the HOMO−1 is clearly attributable to the larger σ-framework of **3b**, which includes the two bridging Si atoms and displays the typical appearance of an oligosilane system (*29*). The lowest unoccupied MO (LUMO) of **3b** is antibonding between the substituent-free silicon atoms, corresponding more closely to the diradical resonance form **C** (Scheme 2), which is in agreement with the longer distance between those atoms calculated for the ^3A_u state of **3b**.

The topology of the total electron density in **3c** (R being Me) was initially probed by Bader's atoms-in-molecules (AIM) method (*30*). This analysis revealed bond critical points (BCPs) for both the annulated three-membered rings and for the central Si_4-motif but not for the long diagonal distance, corroborating the absence of direct bonding between Si1 and Si1′ (interactive table). The value of the electron density ρ(*r*) for $BCP_{Si1\text{-}Si3'}$ [0.078 atomic unit (au)] was higher than for the homobond $BCP_{Si1\text{-}Si3}$ (0.073), which hints at a cyclically delocalized through-bond interaction. An electron localization function (ELF) analysis (*31*) computed for the total electrons shows two disynaptic basins for Si1-Si3/Si1′-Si3′ [1.42 electrons (*e*) each], two further disynaptic basins for Si1-Si3′/Si1′-Si3 (1.96 *e*) and two monosynaptic (nonbonding) basins located on Si1 and Si1′ (1.60 *e*), for which resonance between forms **A** and **B** (Scheme 2) is a fair zero-order representation. The disynaptic basin centroids approximately correspond to the AIM BCPs. If the ELF is restricted to contributions from the top four MOs (dismutative trio plus HOMO−1), the same basin pattern is revealed [with further basins arising from the HOMO−1 (interactive table)]. The total-electron ELF isosurface includes a delocalized

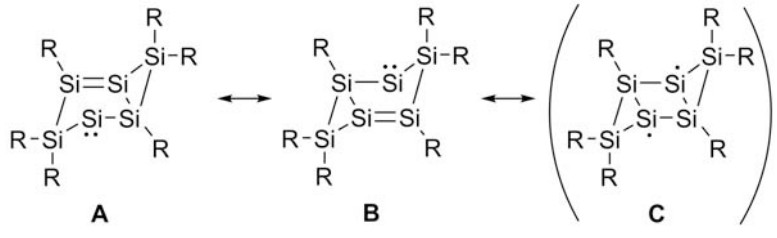

Scheme 2. Resonance formulae (**A**) to (**C**) for **3a-c** [for **3a,** R = Tip; for **3b,** R = Dip (2,6-diisopropylphenyl); for **3c,** R = Me).

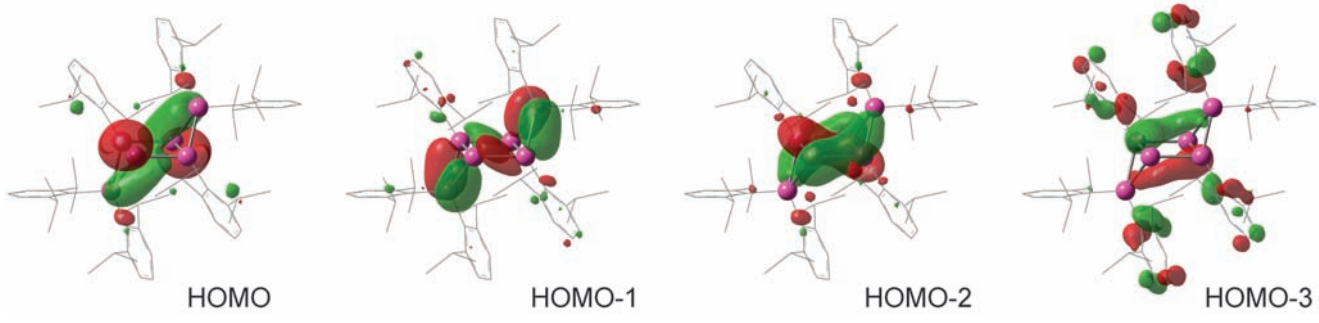

Fig. 2. HOMO, HOMO−1, HOMO−2, and HOMO−3 of model **3b** contoured at 0.035 atomic units (interactive table).

region around the Si_4 ring with a bifurcation threshold (0.755) similar to that reported for homoaromatic carbon rings (*32*). This feature is also present in the ELF isosurface, including just HOMO to HOMO−3. When the HOMO−1 is excluded, the ELF surface now starts to resemble the topology of the torus link computed using the π-MOs of benzene (*33*).

In order to quantify the aromaticity of **3a,b**, we calculated the nucleus-independent chemical shift, NICS(0), at the center of the Si_4 ring of **3b** (−23.8 ppm), which indicates substantial aromaticity (benzene ~ −10 ppm) but may also include shielding effects from the σ-framework (*34*). To estimate these latter effects, we computed the NICS(0) value for **4,** the hypothetical saturated hydrogenation product of **3b**. This in silico reduction has the effect of sequestering the two Si lone pair electrons and hence suppressing the dismutational resonance. The result (−6.4 ppm) suggests that the strongly diatropic NICS(0) value of **3b** is truly due to aromaticity. Further confirmation is obtained from the NICS(0) value of −3.3 ppm for the ^3A_u triplet (and presumed nonaromatic) state of **3b** (resonance **C**) (Scheme 2).

In order to place **3b** in terms of relative energy, we calculated two of its isomers with Dip substituents: the experimentally known hexasilaprismane (*18*) and the hypothetical hexasilabenzene. Both turned out to be lower in free energy ΔG_{298} [B3LYP/6-31G(d); **3b**, 0.0; prismane, −11.7; benzene, −4.3 kcal mol^{-1}] with the hexasilabenzene surprisingly situated midway, which raises the intriguing possibility of a future synthesis of a stable hexasilabenzene.

The general formalism leading to the type of aromaticity exemplified by **3a-c** is a twofold formal 1,2-shift of substituents in the classical Hückel aromatic compounds: a double intramolecular dismutation. The formal oxidation states of the silicon atoms in **3a-c** are +2 (SiR_2), +1 (SiR), and 0 (Si) as opposed to the uniform oxidation state of +1 in hexasilabenzenes. We propose the term dismutational aromaticity for a phenomenon that in principle should be applicable to any classical Hückel aromatic compound with at least six ring atoms.

References and Notes

1. M. Faraday, *Philos. Trans. R. Soc. Lond. B Biol. Sci.* **115**, 440 (1825).
2. W. von E. Doering, F. L. Detert, *J. Am. Chem. Soc.* **73**, 876 (1951).
3. A. T. Balaban, P. R. Schleyer, H. S. Rzepa, *Chem. Rev.* **105**, 3436 (2005).
4. T. C. Dinadayalane, U. D. Priyakumar, G. N. Sastry, *J. Phys. Chem. A* **108**, 11433 (2004).
5. F. A. Cotton, G. Wilkinson, *Advanced Inorganic Chemistry* (Wiley, New York, ed. 4, 1980).
6. R. West, M. J. Fink, J. Michl, *Science* **214**, 1343 (1981).
7. M. Kira, T. Iwamoto, *Adv. Organomet. Chem.* **54**, 73 (2006).
8. A. Sekiguchi, R. Kinjo, M. Ichinohe, *Science* **305**, 1755 (2004).
9. T. Sasamori *et al.*, *J. Am. Chem. Soc.* **130**, 13856 (2008).
10. V. Y. Lee, A. Sekiguchi, *Angew. Chem. Int. Ed.* **46**, 6596 (2007).
11. K. Wakita, N. Tokitoh, R. Okazaki, S. Nagase, *Angew. Chem. Int. Ed.* **39**, 634 (2000).
12. R. Kinjo *et al.*, *J. Am. Chem. Soc.* **129**, 7766 (2007).
13. M. Ichinohe, M. Igarashi, K. Sanuki, A. Sekiguchi, *J. Am. Chem. Soc.* **127**, 9978 (2005).
14. V. Y. Lee, K. Takanashi, T. Matsuno, M. Ichinohe, A. Sekiguchi, *J. Am. Chem. Soc.* **126**, 4758 (2004).
15. M. J. S. Dewar, D. H. Lo, C. H. Ramsden, *J. Am. Chem. Soc.* **97**, 1311 (1975).
16. S. Nagase, H. Teramae, T. Kudo, *J. Chem. Phys.* **86**, 4513 (1987).
17. K. K. Baldridge, O. Uzan, J. M. L. Martin, *Organometallics* **19**, 1477 (2000).
18. A. Sekiguchi, T. Yatabe, C. Kabuto, H. Sakurai, *J. Am. Chem. Soc.* **115**, 5853 (1993).
19. K. Abersfelder, D. Scheschkewitz, *J. Am. Chem. Soc.* **130**, 4114 (2008).
20. D. Scheschkewitz, *Angew. Chem. Int. Ed.* **44**, 2954 (2005).
21. D. Scheschkewitz, *Angew. Chem. Int. Ed.* **43**, 2965 (2004).
22. Materials and methods are available as supporting material on *Science* Online and contain details of experimental procedures, analytical data, and x-ray structure determinations. Details of the computational procedures are available via the interactive table and the digital repository links therein. Regarding general information on the digital repository, see (*35*).
23. L. Shimoni-Livny, J. P. Glusker, C. W. Bock, *Inorg. Chem.* **37**, 1853 (1998).
24. A. Schnepf, *Chem. Soc. Rev.* **36**, 745 (2007).
25. G. Fischer *et al.*, *Angew. Chem. Int. Ed.* **44**, 7884 (2005).
26. Q. Zhang *et al.*, *J. Am. Chem. Soc.* **131**, 9789 (2009).
27. E. Niecke, A. Fuchs, F. Baumeister, M. Nieger, W. W. Schoeller, *Angew. Chem. Int. Ed. Engl.* **34**, 555 (1995).
28. M. Seierstad, C. R. Kinsinger, C. J. Cramer, *Angew. Chem. Int. Ed.* **41**, 3894 (2002).
29. T. Schepers, J. Michl, *J. Phys. Org. Chem.* **15**, 490 (2002).
30. R. F. W. Bader, *Atoms in Molecules: A Quantum Theory* (Oxford Univ. Press, Oxford, 1990).
31. A. Savin *et al.*, *Angew. Chem. Int. Ed. Engl.* **31**, 187 (1992).
32. C. S. M. Allan, H. S. Rzepa, *J. Chem. Theory Comput.* **4**, 1841 (2008).
33. C. S. Wannere *et al.*, *J. Phys. Chem. A* **113**, 11619 (2009).
34. Z. Chen, C. S. Wannere, C. Corminboeuf, R. Puchta, P. R. Schleyer, *Chem. Rev.* **105**, 3842 (2005).
35. J. Downing *et al.*, *J. Chem. Inf. Model.* **48**, 1571 (2008).

36. We thank the Deutsche Forschungsgemeinschaft (DFG SCHE 906/3-2) and the Karl-Winnacker-Fund of the Aventis Foundation for financial support. Crystallographic details were deposited with the Cambridge Crystallographic Data Centre as CCDC-745660 (**2**) and 745661 (**3a**).

Supporting Online Material

www.sciencemag.org/cgi/content/full/327/5965/564/DC1
Materials and Methods
Figs. S1 to S6
Reference
Interactive Table

10 September 2009; accepted 24 November 2009
10.1126/science.1181771

Combined Effects on Selectivity in Fe-Catalyzed Methylene Oxidation

Mark S. Chen and M. Christina White*

Methylene C–H bonds are among the most difficult chemical bonds to selectively functionalize because of their abundance in organic structures and inertness to most chemical reagents. Their selective oxidations in biosynthetic pathways underscore the power of such reactions for streamlining the synthesis of molecules with complex oxygenation patterns. We report that an iron catalyst can achieve methylene C–H bond oxidations in diverse natural-product settings with predictable and high chemo-, site-, and even diastereoselectivities. Electronic, steric, and stereoelectronic factors, which individually promote selectivity with this catalyst, are demonstrated to be powerful control elements when operating in combination in complex molecules. This small-molecule catalyst displays site selectivities complementary to those attained through enzymatic catalysis.

Methylene (secondary) C–H bonds are ubiquitous in organic structures and are often viewed by organic chemists as the inert scaffold upon which the traditional chemistry of "reactive" functional groups is performed. In contrast, the enzymatic oxidation of methylenes (i.e., C–H to C–O) is a fundamental transformation in biological systems and is critical for drug metabolism and the biosynthesis of secondary metabolites (*1*, *2*). Selectivity in enzymatic catalysis is dictated by the local chemical environment of the enzyme active site, a feature that inherently limits substrate scope. Despite important advances in the discovery of catalysts for C–H oxidation, the ability to directly functionalize isolated, unactivated secondary C–H bonds with useful levels of selectivity in complex molecule settings under preparatively useful conditions (i.e., limiting amounts of substrate) has been restricted to the realm of enzymatic catalysis. A small-molecule catalyst capable of performing methylene oxidations with broad scope, predictable selectivities, and in preparatively useful yields would have a transformative effect on streamlining the practice of organic synthesis.

The paucity of methods for the oxidation of isolated, unactivated, and nonequivalent secondary C–H bonds underscores that they are, arguably, the most challenging chemical bonds to selectively functionalize. Reactivity for oxidizing such bonds had been observed with several catalysts, but generally in substrates where selectivity issues are circumvented (e.g., cyclohexane → cyclohexanone) (*3*–*11*) or else where reactive sites are either electronically activated (i.e., adjacent

Department of Chemistry, Roger Adams Laboratory, University of Illinois, Urbana, IL 61801, USA.

*To whom correspondence should be addressed. E-mail: white@scs.uiuc.edu